ISSN 0021-3640, JETP Letters, 2023, Vol. 117, No. 5, pp. 339–343. © The Author(s), 2023. This article is an open access publication.
Russian Text © The Author(s), 2023, published in Pis'ma v Zhurnal Eksperimental'noi i Teoreticheskoi Fiziki, 2023, Vol. 117, No. 5, pp. 344–349.

OPTICS
AND LASER PHYSICS

Observation of Spatiotemporal Self-Compression of Pulses in One-Dimensional Waveguide Arrays Fabricated by Laser Writing

A. A. Arkhipova[a,b], S. A. Zhuravitskii[a,c], N. N. Skryabin[a,c], I. V. D'yakonov[a,c], A. A. Kalinkin[a,c], S. P. Kulik[c], S. V. Chekalin[a], Ya. V. Kartashov[a], B. N. Zadkov[a], and V. O. Kompanets[a,*]

[a] *Institute of Spectroscopy, Russian Academy of Sciences, Troitsk, Moscow, 108840 Russia*
[b] *National Research University Higher School of Economics, Moscow, 101000 Russia*
[c] *Quantum Technology Center, Faculty of Physics, Moscow State University, Moscow, 119991 Russia*
**e-mail: kompanetsvo@isan.troitsk.ru*

Received January 12, 2023; revised January 27, 2023; accepted January 28, 2023

The features of nonlinear propagation of high-intensity pulses in the short-wavelength infrared range in extended one-dimensional waveguide arrays with different spatial periods, formed in fused silica by laser writing, are studied. More than tenfold self-compression of femtosecond pulses up to a duration of several periods of the light field is experimentally observed.

DOI: 10.1134/S0021364023600179

1. INTRODUCTION

One of the most interesting phenomena in nonlinear optics is the self-action of high-intensity radiation propagating in media with the Kerr nonlinearity. Of particular interest is the situation where the wave packet is localized both in space and time as a result of an exact balance between the focusing nonlinearity of the medium, diffraction, and anomalous dispersion, and so-called light bullets, i.e., three-dimensional soliton states propagating in a nonlinear medium without distortion, are formed [1]. However, these states are dynamically unstable in a homogeneous cubic nonlinear medium and can collapse or spread, depending on the type of perturbations that cause the development of instability [1]. In this case, a strong temporal compression of the pulse at the initial stages of collapse can lead to a very significant influence of higher order temporal effects—higher order dispersion, the Raman effect, pulse self-steepening, etc.—on the subsequent evolutionary dynamics. As a result, the spatiotemporal localization of light bullets propagating in an isotropic condensed medium is usually observed only over fractions of a millimeter, after which these states are destroyed [2]. However, in spatially inhomogeneous focusing media of certain configurations, such as photonic crystal fibers or waveguide arrays with a small modulation depth of the refractive index, this distance can be strongly increased, since the transverse periodic modulation of the refractive index of the medium has a stabilizing effect and can suppress collapse even for three-dimensional wave packets, as shown in [3–5]. The nonlinear propagation of long pulses in such media can be accompanied by their significant self-compression (by a factor of 10–100 according to theoretical predictions) [6, 7].

One of the most important properties of these media is the possibility of forming stable three-dimensional light bullets in them that propagate without distortion over fairly large distances; see reviews [8–10]. The growing interest in the propagation of radiation and its spatiotemporal localization in inhomogeneous (including periodic) optical structures with a small modulation depth of the refractive index is associated primarily with significant progress in their fabrication technologies, which include laser writing methods [11], methods in which hollow regions in fiber-type photonic crystals are filled with nonlinear materials with refractive indices close to the refractive index of the fiber material [12], various technologies for the formation of multimode or structured optical fibers [13], and many others, which makes it possible to implement almost arbitrary arrays up to 15–20 cm long. Thus, three-dimensional fundamental [12] and vortex [14] light bullets were first demonstrated in honeycomb waveguide arrays (fabricated on the basis of fiber-type photonic crystals). The possibility of manufacturing optical splitters based on waveguide arrays with different structures, switches, and spatial multiplexers [15], as well as the rapid development of topological photonics in waveguide systems, opens up new prospects for monitoring and controlling the spatiotemporal localization of light in such structures [16]. At the same time, the design of complex waveguide systems that potentially maintain stable spatiotemporal nonlinear states requires the optimization of

the influence of nonlinearity not only on the spatial but also on the temporal transformation of the wave packet. In this work, we experimentally study the features of the transformation of the spatiotemporal structure of radiation in one-dimensional waveguide arrays fabricated in fused silica by laser writing. The spatiotemporal localization in such written one-dimensional structures at wavelengths corresponding to the anomalous group velocity dispersion regime has not yet been experimentally studied; therefore, its observation opens new horizons for studying the propagation of wave packets in a wide range of static and dynamic arrays (including topologically nontrivial structures), which can be produced using this technology. We observe a significant self-compression of pulses during their simultaneous spatial localization, which indicates the potential possibility of the formation of light bullets in one-dimensional waveguide arrays.

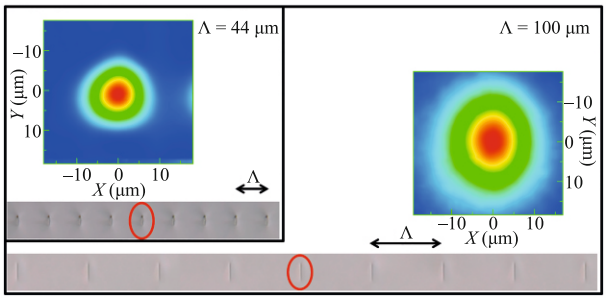

Fig. 1. (Color online) Dimensions of the output waveguide mode and micrographs of the sample ends (main figure) for a low-contrast waveguide array ($\Delta n = 4.2\times10^{-4}$) with a period of 100 μm and (inset) for a high-contrast waveguide array ($\Delta n = 1.3\times10^{-3}$) with a period of 44 μm. The circle marks the waveguide excited in the experiments in the array.

2. EXPERIMENT

To fabricate one-dimensional waveguide arrays, we used femtosecond laser writing technology. The waveguides were inscribed in a JGS1 fused silica sample 100 mm long by focused pulses of the second harmonic of an Antaus (Avesta) fiber laser (wavelength of 515 nm, pulse duration of 280 fs, repetition rate of 1 MHz). During writing, the sample was moved with respect to the focus at a constant speed using a high-precision positioning system (Aerotech); as a result, sets of identical parallel waveguides with controlled interwaveguide distances (periods) were written. To study the effect of waveguide parameters on the spatiotemporal localization of pulses, two one-dimensional arrays of nine waveguides with different refractive index contrasts were fabricated. The first waveguide array with a high contrast (anisotropic change of $\Delta n = 1.3\times10^{-3}$ estimated from the mode size, propagation loss of 0.8 dB/cm) was written by focusing with an aspherical lens with a numerical aperture of NA = 0.55 (strong focusing), pulse energy of 175 nJ, and writing speed of 1 mm/s, and the second array with a low contrast (almost isotropic change estimated at $\Delta n = 4.2\times10^{-4}$, propagation loss of 0.3 dB/cm) was written by focusing with an aspherical lens with a numerical aperture of NA = 0.4 (weak focusing), pulse energy of 400 nJ, and writing speed of 0.25 mm/s. The periods of the arrays were chosen so that the coupling constants between adjacent waveguides had the same value of $C = 0.25$ cm^{-1} (here, the coupling constant defines the power coupling length $L = \pi/2C$ from the excited waveguide to the adjacent one if there are only two waveguides, while in a periodic array it determines the discrete diffraction rate [16] for a single-channel excitation). Since the diameter of the waveguide mode field decreases with increasing contrast, and the coupling constant is determined by the overlap of the modes of adjacent waveguides, to achieve the same coupling constants in two arrays, the pre-calibrated periods were 44 and 100 μm for an array with high and low contrast, respectively. Micrographs of two arrays are shown in Fig. 1 together with the corresponding experimental mode profiles of the waveguides that compose these structures.

To study the propagation of infrared radiation in these arrays, a linearly polarized signal wave of a TOPAS (Light Conversion) parametric amplifier with a tuning range of 1240–1600 nm, a pulse duration of 40–80 fs at an energy of up to 300 μJ, and a pulse repetition rate of 1 kHz was used. To obtain the maximum spatial localization of the wave packet in the arrays under study in the range of initial durations of 100–1000 fs in the focal plane of a single-grating 4*f* stretcher compressor in the linear chirp compensation regime, the spectral width of the radiation was varied using an amplitude mask or an adjustable slit. The output distribution was recorded with an infrared InGaAs camera, and the input and output radiation durations were measured with an ASF-20 single-pulse autocorrelator (Avesta), while the spectra were recorded with an ATP8000 InGaAs spectrometer (Optosky). The cross-correlation recording system [17, 18] described in detail in [12] was used to record the spatiotemporal distribution at the output of waveguide arrays. In this scheme, using a broadband reflecting splitter, the output infrared radiation was combined in the β-barium borate crystal 10 μm thick collinearly with the 45-fs reference radiation of the Ti:sapphire system. The variation of the delay between the 800-nm reference pulses and the studied infrared pulses made it possible to obtain the distribution of the sum frequency generation intensity with their temporal cross-correlation on a CCD camera behind the crystal. The use of a thin crystal with a wide phase matching to generate the sum frequency and the use of an intense reference pulse

make it possible to record the spatiotemporal dynamics of infrared pulses in a wide spectral range at output energies not exceeding a few nanojoules in each waveguide.

3. RESULTS

Spatiotemporal localization of light in our arrays is possible because the focusing Kerr nonlinearity of fused silica simultaneously suppresses diffraction in space and dispersive spreading in time in the anomalous group velocity dispersion regime under refraction in a nonuniform refractive index profile (thus, spatial and temporal evolutions are coupled because of the nonlinearity of the material). The transverse modulation of the refractive index qualitatively changes the character of wave packet diffraction at low energies. In this regime, the overlap of the wave fields of modes in adjacent waveguides leads to the energy transfer between them or to discrete diffraction, which is manifested in the formation of two divergent spatial intensity maxima. In this case, the low-energy pulse is spread in time, remaining bell-shaped at any spatial point. The discrete diffraction rate is determined by the coupling constant and, therefore, it was almost the same in the two written arrays. This can be seen from the bottom row of Fig. 2 (see distributions for 30 nJ), which shows the experimentally measured profiles of the output infrared radiation from the high- and low-contrast arrays when focusing 1400-nm femtosecond radiation into the central waveguide, which lies in the region of weak anomalous dispersion of silica. As the pulse energy increases, the self-action, which is most pronounced near the center of the pulse, leads to a nonlinear self-induced "defect" in the periodic array, which slows down spatial diffraction in the most intense parts of the pulse, while the discrete diffraction rate remains the same at low-intensity pulse tails. As a result, in the integral (time-averaged) spatial distributions shown in Fig. 2, one can see an increase in the concentration of light in the central waveguide with the pulse energy in the presence of initially quite pronounced tails, which are typical of a discrete diffraction pattern. When certain threshold energy values are reached (250 and 1400 nJ in the high- and low-contrast arrays, respectively), the nonlinear spatial localization begins to be manifested quite sharply, similar to that observed in Ge-doped square waveguide arrays technologically embedded in a fused silica substrate [19]. It should be noted that the temporal compression of pulses in our system is maximal at energy levels corresponding to the beginning of the spatial localization (see Fig. 3).

A further increase in the energy leads to a strong localization of radiation almost entirely in one excited waveguide (upper distributions in Fig. 2 for energies of 1300 and 1700 nJ). Despite the same discrete diffraction rates in arrays with different contrasts at low input pulse energies, the nonlinear propagation in them differs significantly. The threshold for localization for waveguides with high contrast is much lower apparently because the waveguide mode in this case is significantly smaller (Fig. 1), which leads to a larger effective nonlinear addition to the refractive index at the same pulse energy. At the same time, the maximum degree of spatial localization that can be achieved in the high-contrast waveguide array is somewhat lower because of high losses (which can also be due to some degradation of the nonlinear coefficient n_2 of the material under strong focusing during the writing of waveguides). It should be noted that the optimal pulse duration to achieve the maximum degree of localization in arrays with a high refractive index contrast was 500–750 fs, and the degree of time compression did not exceed 4. When radiation propagates in a low contrast array, the optimal duration of input pulses for the localization at a wavelength of 1400 nm was 252 fs. Despite a rather high nonlinear localization threshold, a noticeably larger part of the radiation is concentrated in the central waveguide (see Fig. 2, energy of 1700 nJ).

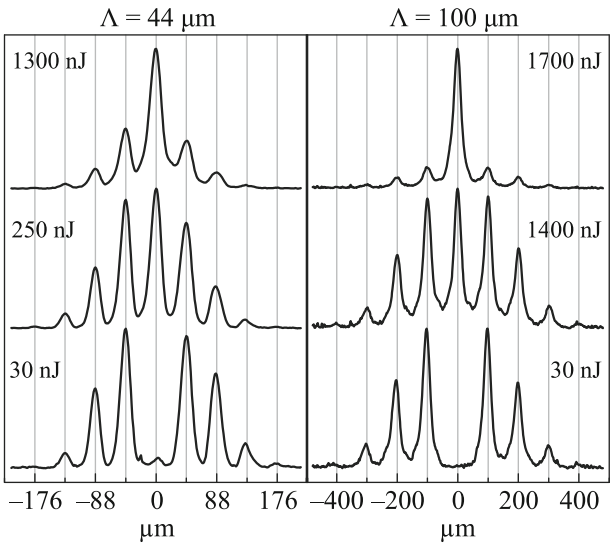

Fig. 2. Output intensity distributions from arrays with (left) high $\Delta n = 1.3 \times 10^{-3}$ and (right) low $\Delta n = 4.2 \times 10^{-4}$ contrast at linear propagation (30 nJ), at the localization threshold (250 and 1400 nJ), and at the maximum degree of spatial localization (1300 and 1700 nJ).

To study the spectral and temporal evolution (Fig. 3), a diaphragm 100 μm in diameter, which transmitted radiation only from the central waveguide, was installed at the exit from the sample. The measurement results demonstrate the dynamics of pulse spectrum broadening simultaneously with the redshift caused by self-induced Raman scattering with an increase in the input pulse energy (Fig. 3, left). In this case, temporal pulse compression occurs in the central waveguide (Fig. 3, right). At an input energy of

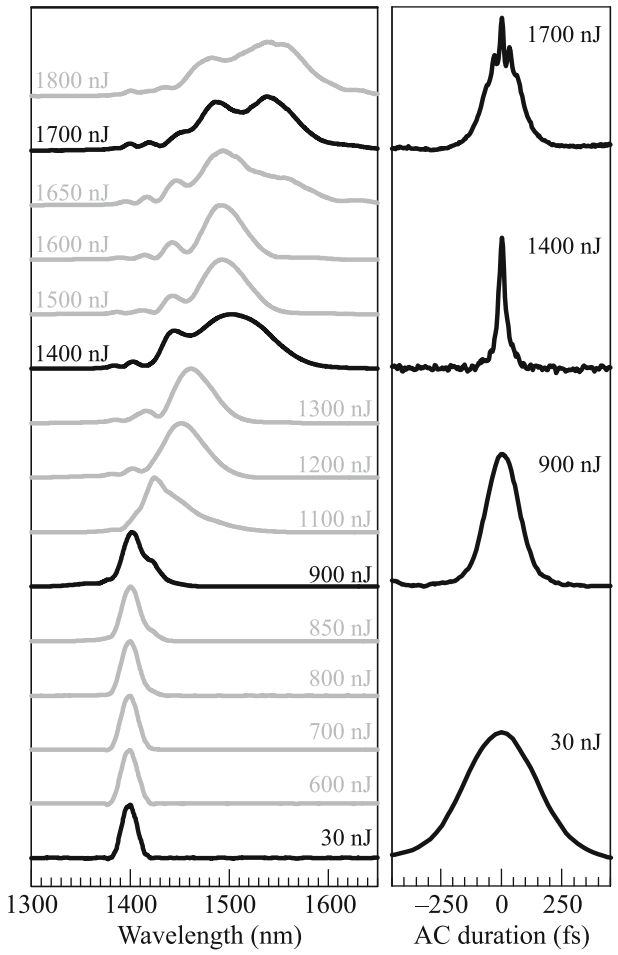

Fig. 3. (Left) Normalized spectra and (right) autocorrelation functions of pulses at the output of the central channel of a low-contrast waveguide array measured at the specified input energies.

1400 nJ, the FWHM duration of the output pulse had a minimum value of 20.2 fs, which corresponds to four field oscillation cycles at a wavelength of 1500 nm and is at the lower limit of the time resolution of the ASF-20 autocorrelator. Thus, the pulse passing through the low-contrast waveguide array is self-compressed by more than an order of magnitude. The recorded pulse duration in the side channels coincided with the input (252 fs) up to energies of 500 nJ. A further increase in the energy leads to a sharp increase in the spatial localization, when the energy is almost completely concentrated in one channel, while the pulse can be broken into several pulses as a result of the development of modulations on the initial wide temporal envelope. The first temporal localization point, which can be associated with the formation of a light bullet, appears in the central waveguide at the exit from the sample (see the autocorrelation function in Fig. 3 at 1400 nJ). With a further increase in the energy, the second, third, etc., light bullets are formed (Fig. 3 at 1700 nJ) in agreement with the numerical simulation in [20].

The spatiotemporal dynamics measured by the cross-correlation method in the waveguide array under study for energy levels corresponding to quasi-linear spreading, the localization threshold, and the maximum degree of spatial localization is shown in Fig. 4. Zero delay between the linearly diffracted infrared pulse and the 45-fs reference pulse of the Ti:sapphire laser system is highlighted in red. The left panel of Fig. 4 shows the linear spatiotemporal distribution of radiation at the exit from the array. The duration of the infrared pulse reconstructed from the cross-correlation for each individual waveguide is 250 fs and almost coincides with the input duration. The middle panel of Fig. 4 clearly shows the evolution of the pulse at the spatial localization threshold. The compression of radiation in time in the side waveguides begins before approximately 100 fs, while compression in the central channel is much more pronounced and occurs later in time. Cross-correlation measurements with a smaller delay step showed that the duration at the output of the central waveguide does not exceed 27 fs with

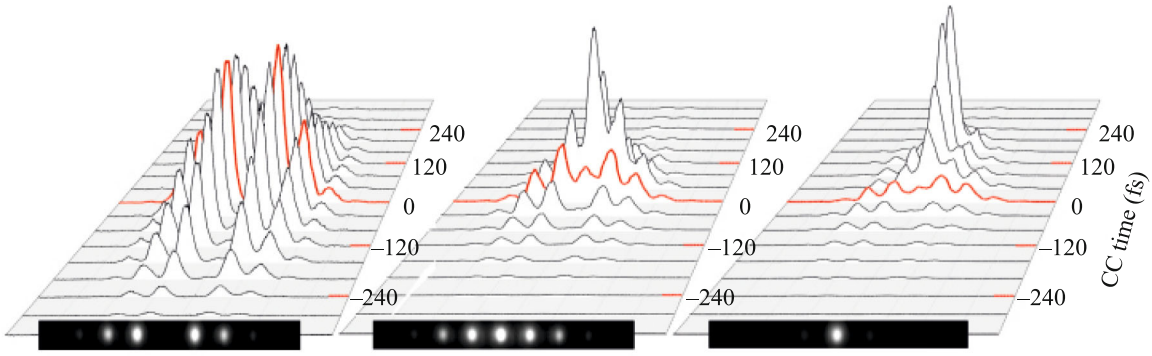

Fig. 4. (Color online) Cross-correlation measurements of the output radiation from an array with $\Delta n = 4.2 \times 10^{-4}$ depending on the input energy of infrared pulses (left) for linear propagation at 200 nJ, (middle) at a localization threshold of 1400 nJ, and (right) for the maximum localization at 1700 nJ. The red line marks zero delay between the reference and test pulses. The bottom row shows the corresponding images of the output profiles on an infrared camera.

a Raman delay of several tens of femtoseconds. With a further increase in the energy of the input pulses, nonlinear temporal localization with the steepening of the trailing edge of the pulse and a Raman delay similar to that observed in [21] are seen.

4. CONCLUSIONS

We have demonstrated strong spatiotemporal compression of infrared radiation, which lies in the region of weak anomalous group velocity dispersion, in waveguide arrays fabricated by femtosecond laser writing inside fused silica. At temporal compression without additional dispersive post-compression by more than an order of magnitude, pulses reach a duration of a few field oscillation cycles at telecommunication wavelengths. These results open wide possibilities for the development of waveguide arrays for spectral transformation and temporal compression of microjoule subpicosecond pulses, as well as for further experimental studies of the dynamics of ultrashort pulses in topological switching devices, in particular, the excitation and propagation of stable topological light bullets in systems with complex spatial structures, e.g., dynamic waveguide arrays [22].

FUNDING

This work was supported by the Russian Science Foundation (project no. 21-12-00096) and by the Ministry of Science and Higher Education of the Russian Federation (state assignment no. FFUU-2022-0004).

CONFLICT OF INTEREST

The authors declare that they have no conflicts of interest.

OPEN ACCESS

REFERENCES

1. Y. Silberberg, Opt. Lett. **15**, 1282 (1990).
2. E. D. Zaloznaya, A. E. Dormidonov, V. O. Kompanets, S. V. Chekalin, and V. P. Kandidov, JETP Lett. **113**, 787 (2021).
3. A. B. Aceves, C. de Angelis, A. M. Rubenchik, and S. K. Turitsyn, Opt. Lett. **19**, 329 (1994).
4. A. B. Aceves, G. G. Luther, C. de Angelis, A. M. Rubenchik, and S. K. Turitsyn, Phys. Rev. Lett. **75**, 73 (1995).
5. D. Mihalache, D. Mazilu, F. Lederer, Y. V. Kartashov, L.-C. Crasovan, and L. Torner, Phys. Rev. E **70**, 055603(R) (2004).
6. A. A. Balakin, S. A. Skobelev, A. V. Andrianov, N. A. Kalinin, and A. G. Litvak, Opt. Lett. **44**, 5085 (2019).
7. M. Rehan, G. Kumar, V. Rastogi, D. A. Korobko, and A. A. Sysolyatin, Laser Phys. **29**, 025104 (2019).
8. B. A. Malomed, D. Mihalache, F. Wise, and L. Torner, J. Opt. B **7**, R53 (2005).
9. B. A. Malomed, Eur. Phys. J. Spec. Top. **225**, 2507 (2016).
10. D. Mihalache, Rom. Rep. Phys. **69**, 403 (2017).
11. K. M. Davis, K. Miura, N. Sugimoto, and K. Hirao, Opt. Lett. **21**, 1729 (1996).
12. S. Minardi, F. Eilenberger, Y. V. Kartashov, A. Szameit, U. Röpke, J. Kobelke, K. Schuster, H. Bartelt, S. Nolte, L. Torner, F. Lederer, A. Tünnermann, and T. Pertsch, Phys. Rev. Lett. **105**, 263901 (2013).
13. W. H. Renninger and F. W. Wise, Nat. Commun. **4**, 1719 (2013).
14. F. Eilenberger, K. Prater, S. Minardi, R. Geiss, U. Röpke, J. Kobelke, K. Schuster, H. Bartelt, S. Nolte, A. Tunnermann, and T. Pertsch, Phys. Rev. X **3**, 041031 (2013).
15. D. N. Christodoulides and E. D. Eugenieva, Phys. Rev. Lett. **87**, 233901 (2001).
16. Y. V. Kartashov, G. E. Astrakharchik, B. A. Malomed, and L. Torner, Nat. Rev. Phys. **1**, 185 (2019).
17. M. A. C. Potenza, S. Minardi, J. Trull, G. Blasi, D. Salerno, P. D. Trapani, A. Varanavicius, and A. Piskarskas, Opt. Commun. **229**, 381 (2004).
18. S. Minardi, J. Trull, and M. A. C. Potenza, J. Hologr. Speckle **5**, 85 (2009).
19. D. Cheskis, S. Bar-Ad, R. Morandotti, J. S. Aitchison, H. S. Eisenberg, Y. Silberberg, and D. Ross, Phys. Rev. Lett. **91**, 223901 (2003).
20. A. A. Balakin, A. G. Litvak, V. A. Mironov, and S. A. Skobelev, Laser Phys. **28**, 045401 (2018).
21. F. Eilenberger, S. Minardi, A. Szameit, U. Röpke, J. Kobelke, K. Schuster, H. Bartelt, S. Nolte, L. Torner, F. Lederer, and A. Tünnermann, Phys. Rev. A **84**, 013836 (2011).
22. C. Milian, Y. V. Kartashov, and L. Torner, Phys. Rev. Lett. **123**, 133902 (2019).

Translated by L. Mosina